

## Supplemental Information

### Emergence of Ruddlesden-Popper Phases and Other Pitfalls for Moderate Temperature Solution Deposited Chalcogenide Perovskites

Apurva A. Pradhan<sup>\*,1</sup>, Shubhanshu Agarwal<sup>\*,1</sup>, Kiruba Catherine Vincent<sup>1</sup>, Daniel C. Hayes<sup>1</sup>, Jonas M. Peterson<sup>2</sup>, Jonathan W. Turnley<sup>1</sup>, Robert M. Spilker<sup>1</sup>, Madeleine C. Uible<sup>2</sup>, Suzanne C. Bart<sup>2</sup>, Libai Huang<sup>2</sup>, Kim Kisslinger<sup>3</sup>, Rakesh Agrawal<sup>1,a)</sup>

<sup>1</sup>Davidson School of Chemical Engineering, Purdue University, West Lafayette, IN 47907, USA

<sup>2</sup>H.C. Brown Laboratory, Department of Chemistry, Purdue University, West Lafayette, IN 47907, USA

<sup>3</sup>Center for Functional Nanomaterials, Brookhaven National Laboratory, Upton, NY 11973, USA

\* Equal Contribution

<sup>a)</sup> Author to whom correspondence should be addressed: [agrawalr@purdue.edu](mailto:agrawalr@purdue.edu)

**Table S1:** The calculated amount of H<sub>2</sub>S, HfS<sub>3</sub>, S, H<sub>2</sub>, HfS<sub>2</sub>, and HfH<sub>2</sub> in each ampule based on the amount of sulfur and HfH<sub>2</sub> loaded into each ampule in Table 1 of the main text.

Sample	Theoretical H <sub>2</sub> S (mmol)	Theoretical HfS <sub>3</sub> (mmol)	Theoretical Sulfur (mmol)	Theoretical H <sub>2</sub> (mmol)	Theoretical HfS <sub>2</sub> (mmol)	Theoretical HfH <sub>2</sub> (mmol)
1	0.03	0.03	0.33	0.00	0.00	0.00
2	0.03	0.03	0.18	0.00	0.00	0.00
3	0.03	0.03	0.03	0.00	0.00	0.00
4	0.00	0.00	0.00	0.03	0.03	0.00
5	0.00	0.00	0.00	0.015	0.015	0.015

**Table S2:** X-ray fluorescence (XRF) measurements of Ba-Zr-S films with varying amounts of sulfur during the sulfurization heat treatment step (shown in Table 1 and Table S1) after a 1 h sulfurization heat treatment at 575 °C averaged over three different spots with three measurements for each spot on each film.

	Ba/Zr	S/Ba	S/Zr	S/(Ba+Zr)
<b>Sample 1</b>	1.40±0.04	3.1±0.1	4.3±0.2	1.81±0.07
<b>Sample 2</b>	1.42±0.04	2.9±0.1	4.0±0.2	1.67±0.06
<b>Sample 3</b>	1.20±0.03	1.82±0.07	2.2±0.1	1.00±0.04
<b>Sample 4</b>	1.44±0.03	1.45±0.06	2.1±0.1	0.86±0.04
<b>Sample 5</b>	1.37±0.05	1.66±0.09	2.3±0.2	0.96±0.06
<b>No Sulfurization Heat Treatment</b>	1.36±0.09	1.71±0.09	2.3±0.3	0.98±0.08

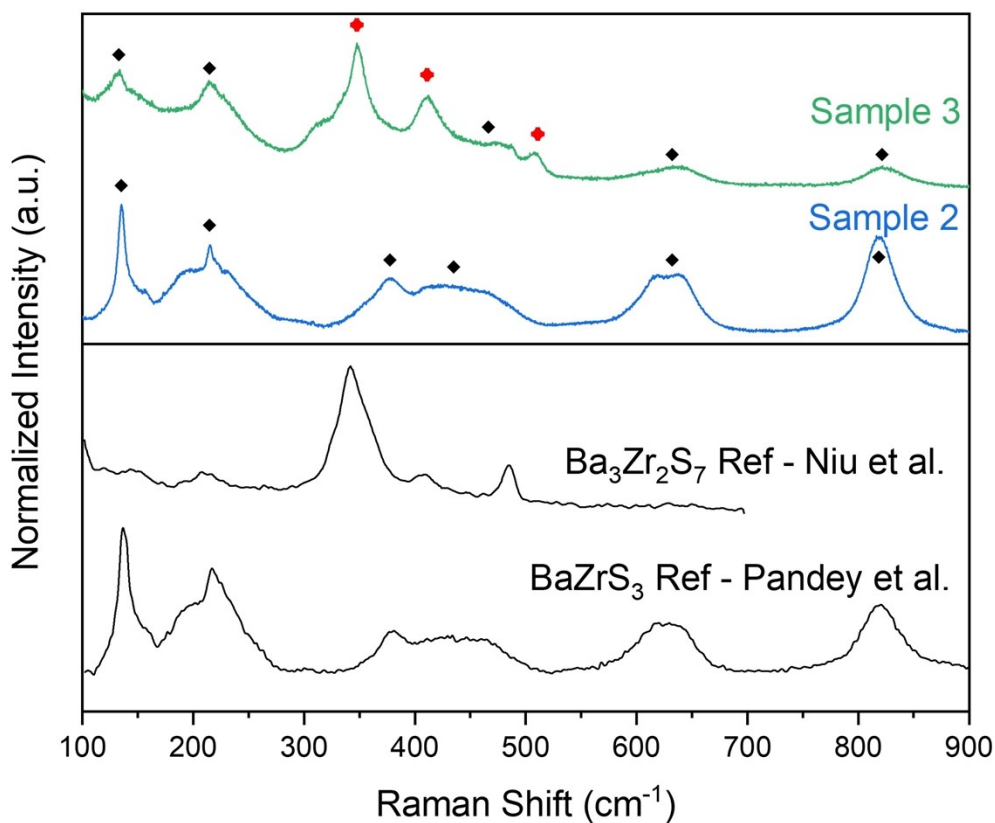


**Figure S1:** Raman spectra for Ba-Zr-S films sulfurized for 1 h at 575 °C with varying amounts of sulfur during the heat treatment step (shown in Table 1 and Table S1). These Raman spectra were taken on individual grains. While Sample 2 matches very well with the spectra for BaZrS<sub>3</sub>, Sample 3 appears to be a mixture of BaZrS<sub>3</sub> and Ba<sub>3</sub>Zr<sub>2</sub>S<sub>7</sub>, indicating that single grains may contain regions of BaZrS<sub>3</sub> and RP phases. Black diamonds indicate BaZrS<sub>3</sub> and red plaque symbols indicate Ba<sub>3</sub>Zr<sub>2</sub>S<sub>7</sub>. The primary peaks for Ba<sub>3</sub>Zr<sub>2</sub>S<sub>7</sub> are shifted slightly higher, which may be caused by distortions resulting from crystalline BaZrS<sub>3</sub> and Ba<sub>3</sub>Zr<sub>2</sub>S<sub>7</sub> existing in the same grain. Raman standards for BaZrS<sub>3</sub> and Ba<sub>3</sub>Zr<sub>2</sub>S<sub>7</sub> were acquired from Pandey et al. and Niu et al., respectively.<sup>1,2</sup>

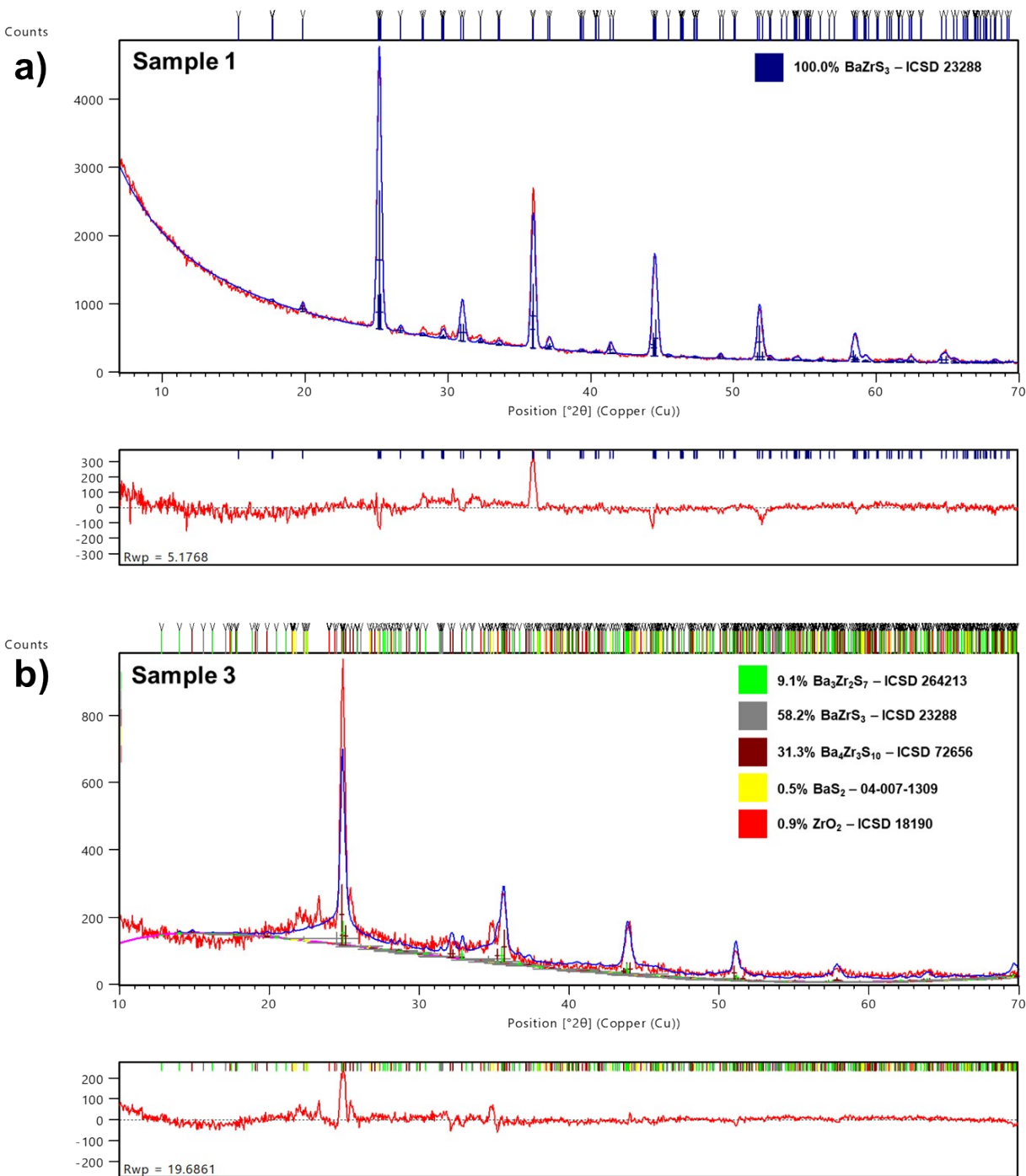


**Figure S2:** Rietveld refinement for Sample 1 and Sample 3 in Figure 1 of the main text. **a)** The pattern collected for Sample 1 is fully accounted for by BaZrS<sub>3</sub> with no unaccounted-for peaks, as shown by Rietveld refinement. **b)** The XRD pattern collected by sample 3 was found to be accounted for by 58.2% BaZrS<sub>3</sub> and a mixture of the RP phases Ba<sub>3</sub>Zr<sub>2</sub>S<sub>7</sub> and Ba<sub>4</sub>Zr<sub>3</sub>S<sub>10</sub>. The formation of these two RP phases together is commonly seen in the literature.<sup>3</sup> Binary phases, including BaS<sub>2</sub>, BaS<sub>3</sub>, and ZrO<sub>2</sub>, accounted for less than two percent of the collected spectra of Sample 3.

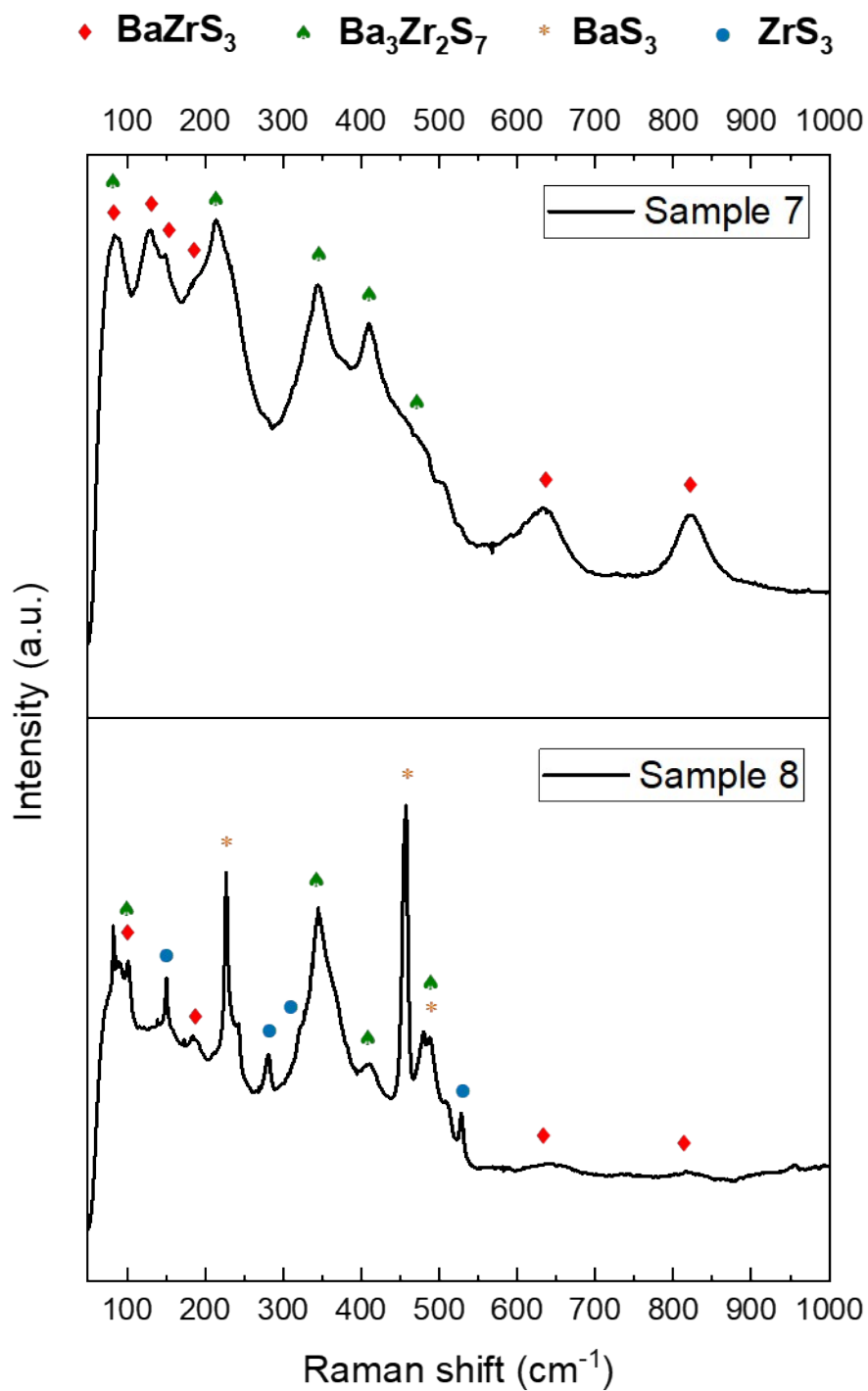


**Figure S3:** Raman spectra for Ba-Zr-S films from hybrid precursor route sulfurized for 15 min at 575 °C with 0.07 atm and 0.03 atm sulfur pressures, respectively. Raman standards for  $\text{BaZrS}_3$  and  $\text{Ba}_3\text{Zr}_2\text{S}_7$  were acquired from Pandey et al. and Niu et al., respectively.<sup>1,2</sup>

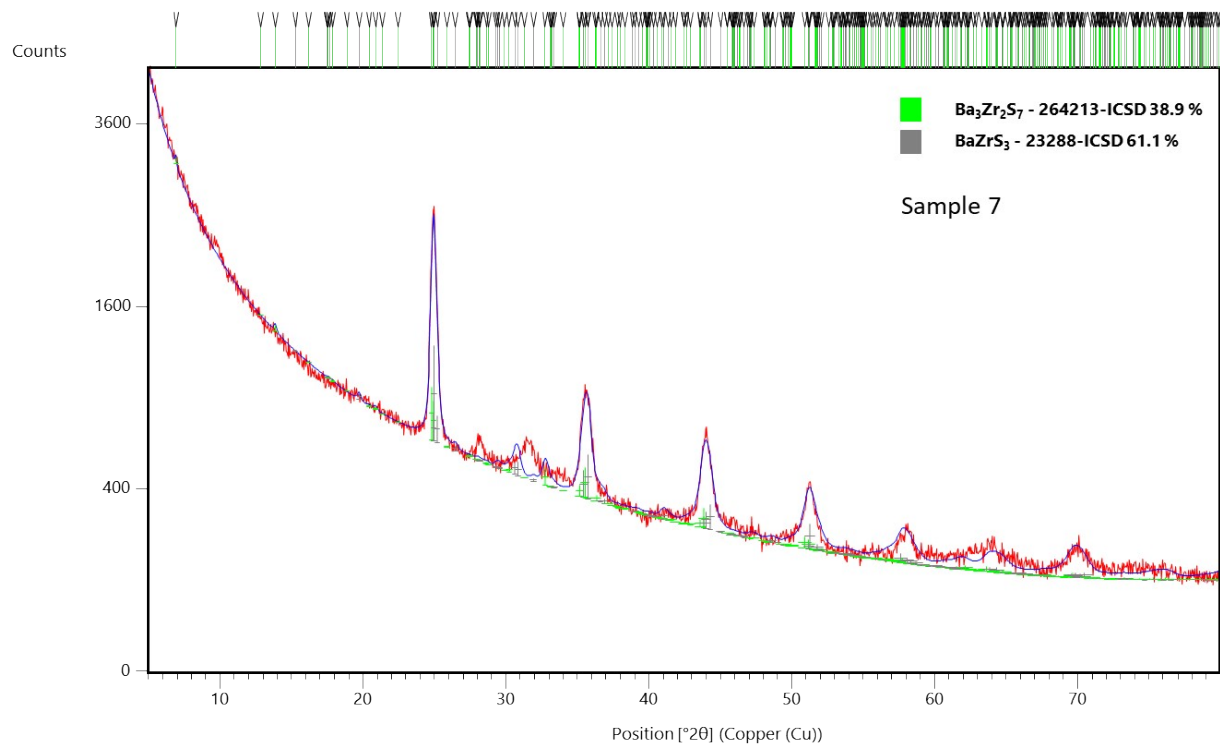


**Figure S4:** Rietveld refinement for Sample 7 synthesized from method 2 described in the main text. The XRD pattern collected was found to be accounted for by 61.1%  $\text{BaZrS}_3$  and 38.9% RP phases  $\text{Ba}_3\text{Zr}_2\text{S}_7$ .

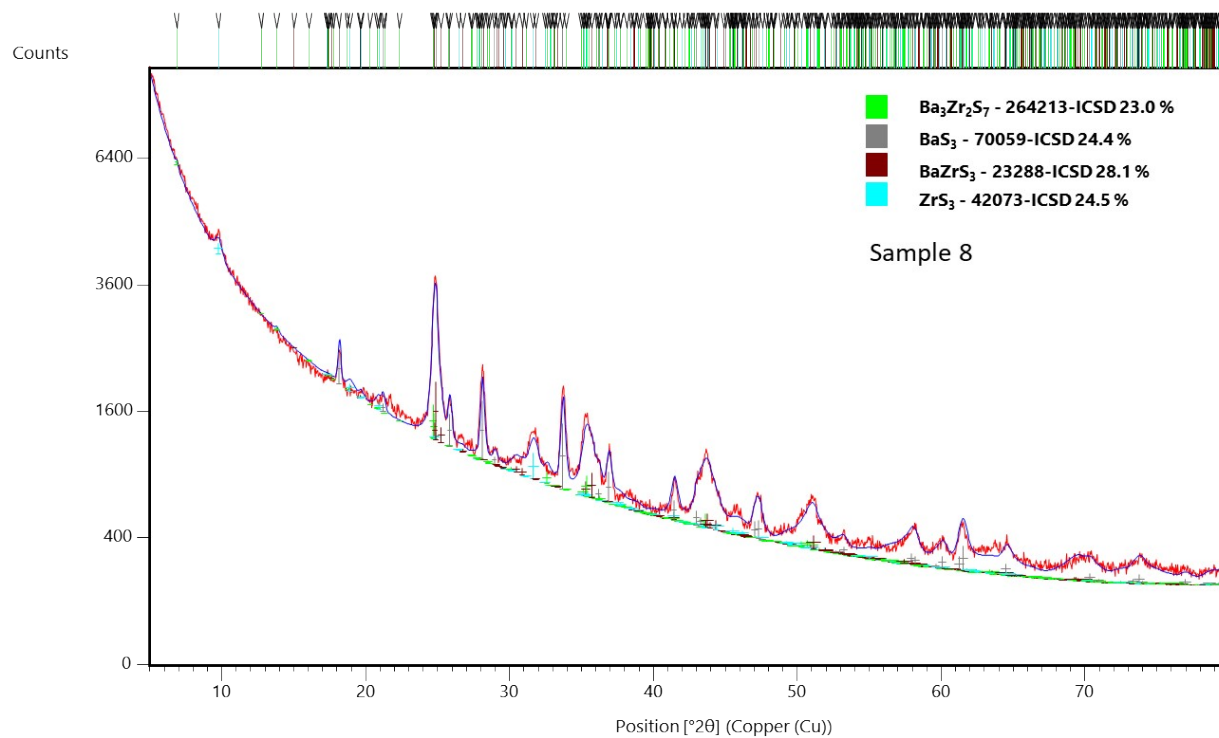


**Figure S5:** Rietveld refinement for Sample 8 synthesized from method 2 described in the main text. The XRD pattern collected was found to be accounted for by 28.1%  $\text{BaZrS}_3$ , 23% RP phases  $\text{Ba}_3\text{Zr}_2\text{S}_7$ , 24.4%  $\text{BaS}_3$ , and 24.5%  $\text{ZrS}_3$ .

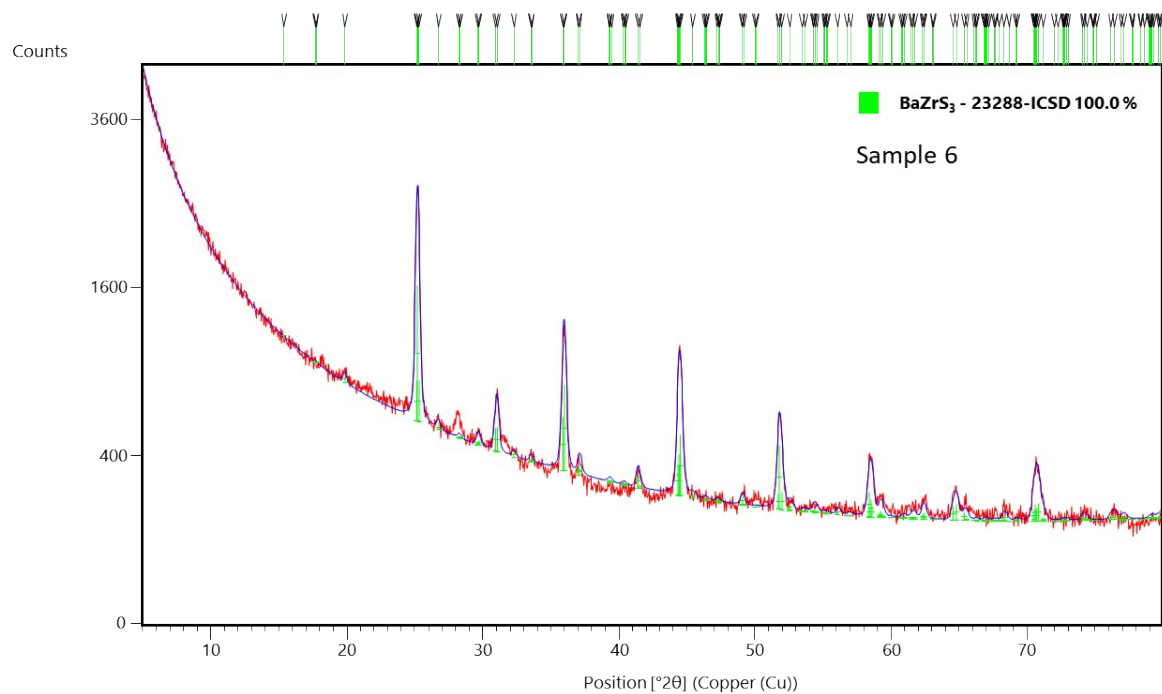


**Figure S6:** Rietveld refinement for Sample 6 synthesized from method 2 described in the main text. The pattern collected is fully accounted for by BaZrS<sub>3</sub> with no unaccounted-for peaks, as shown by Rietveld refinement.

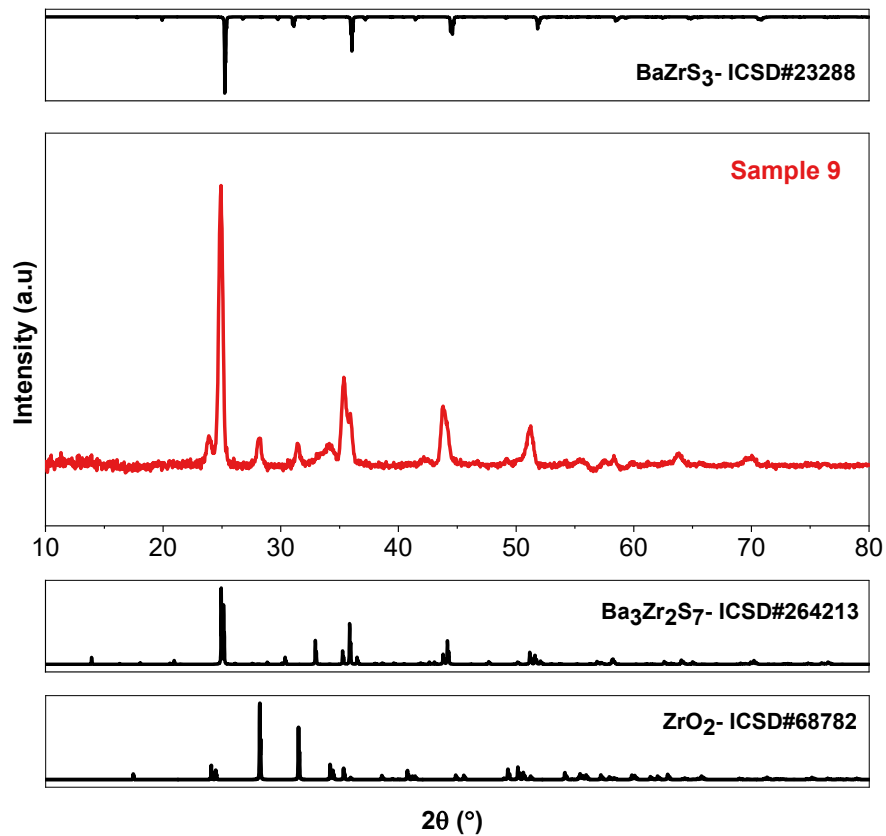


**Figure S7:** XRD pattern for Ba-Zr-S film from hybrid precursor route sulfurized for 24 h at 575 °C with 0.07 atm sulfur pressure.

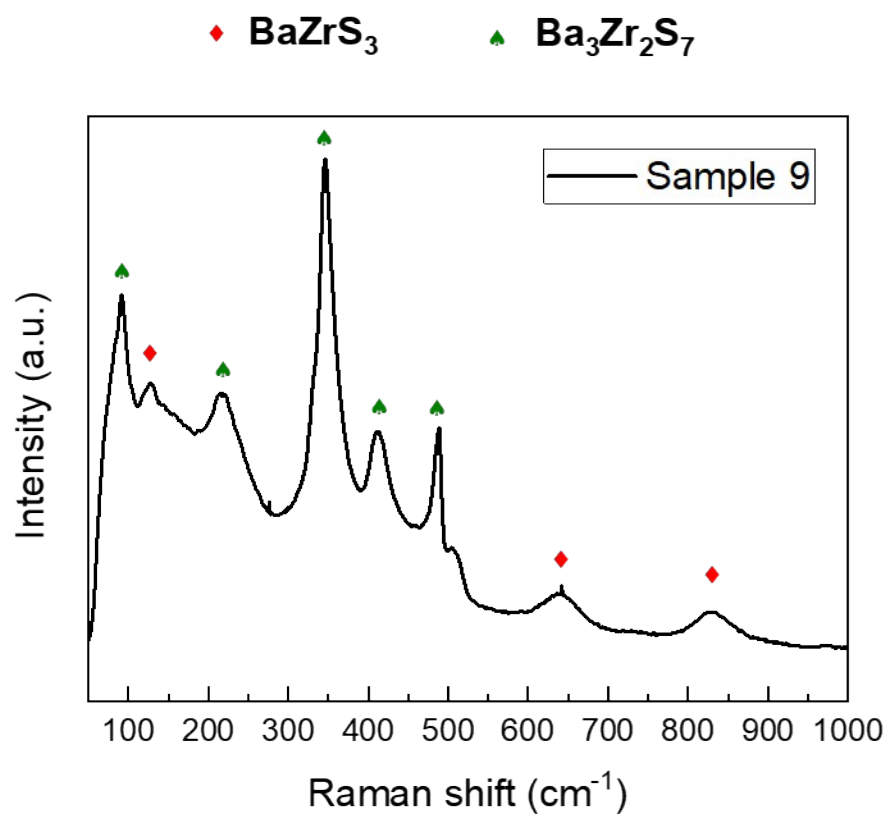


**Figure S8:** Raman spectrum for Ba-Zr-S film from hybrid precursor route sulfurized for 24 h at 575 °C with 0.07 atm sulfur pressure. Raman standards for  $\text{BaZrS}_3$  and  $\text{Ba}_3\text{Zr}_2\text{S}_7$  were acquired from Pandey et al. and Niu et al., respectively.<sup>1,2</sup>

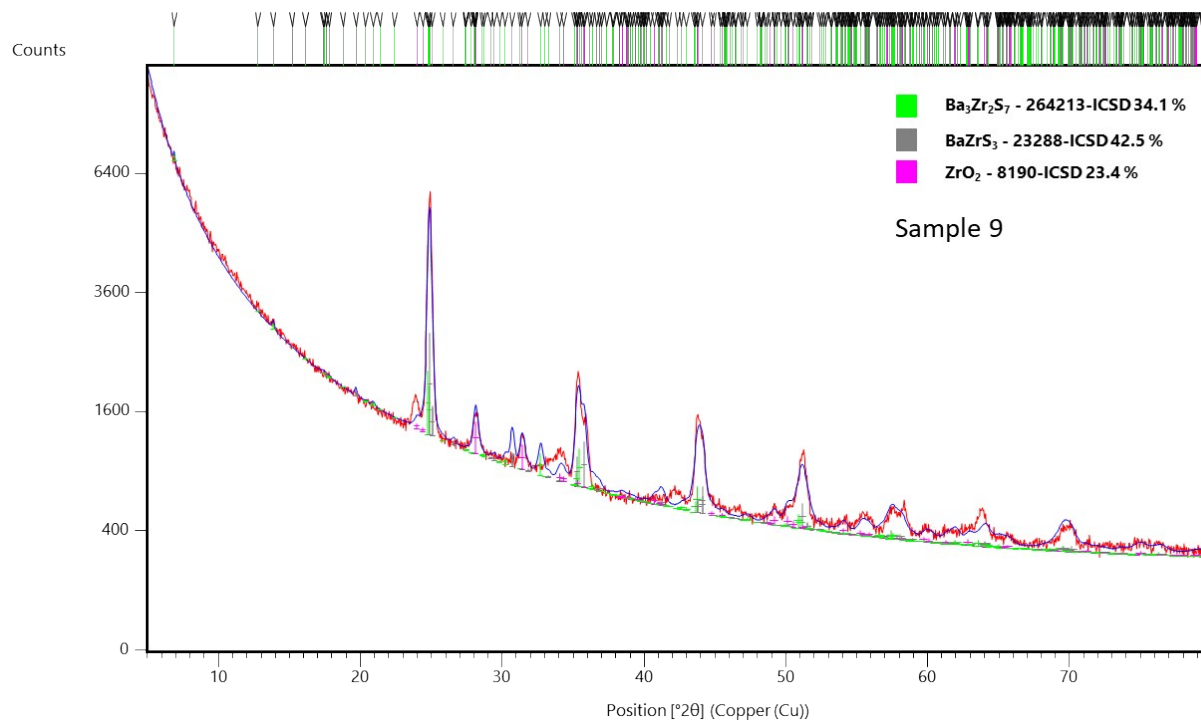


**Figure S9:** Rietveld refinement for Sample 9 synthesized from method 2 described in the main text. The XRD pattern collected was found to be accounted for by 42.5%  $\text{BaZrS}_3$ , 34.1% RP phases  $\text{Ba}_3\text{Zr}_2\text{S}_7$  and 23.4%  $\text{ZrO}_2$ .

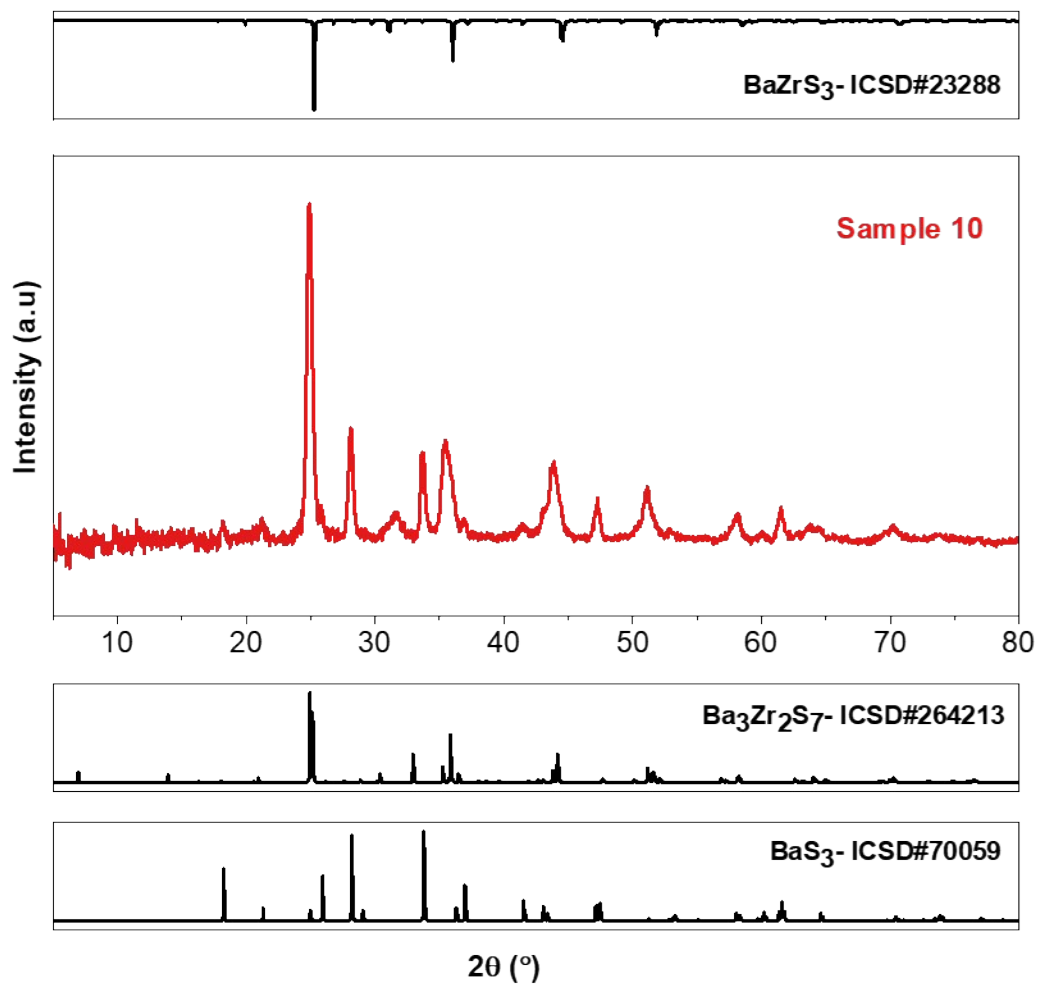


**Figure S10:** XRD pattern for Ba-Zr-S film from hybrid precursor route sulfurized for 15 min at 575 °C with 0.07 atm sulfur pressure and Ba:Zr 1.5:1.

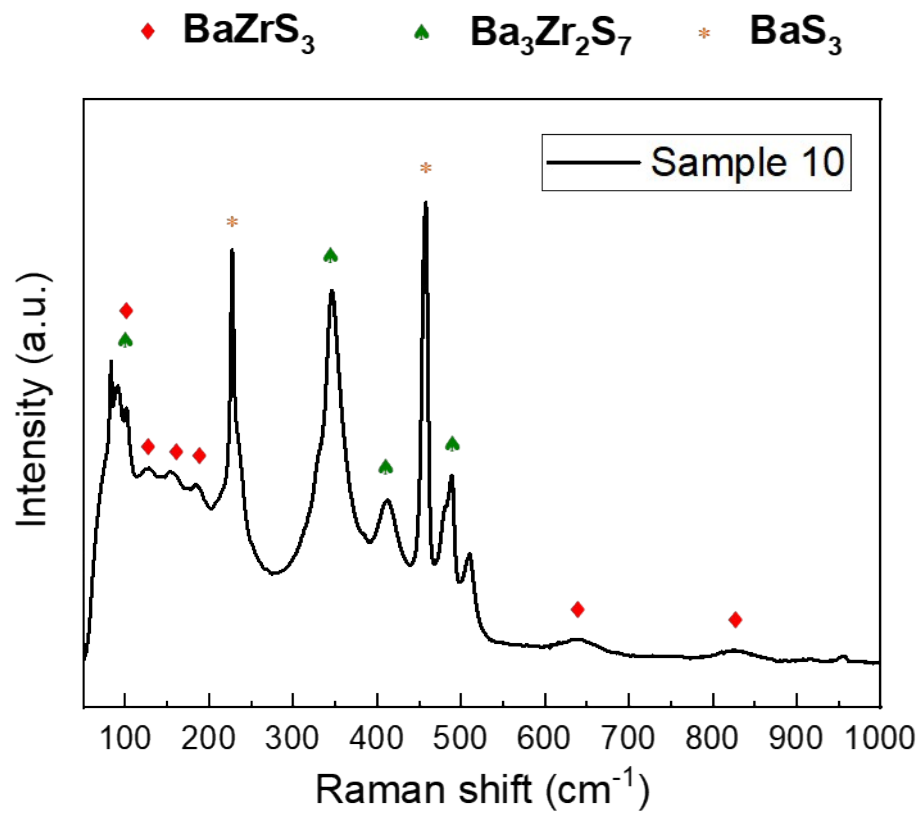


**Figure S11:** Raman spectrum for Ba-Zr-S film from hybrid precursor route sulfurized for 15 min at 575 °C with 0.07 atm sulfur pressure and Ba:Zr 1.5:1.

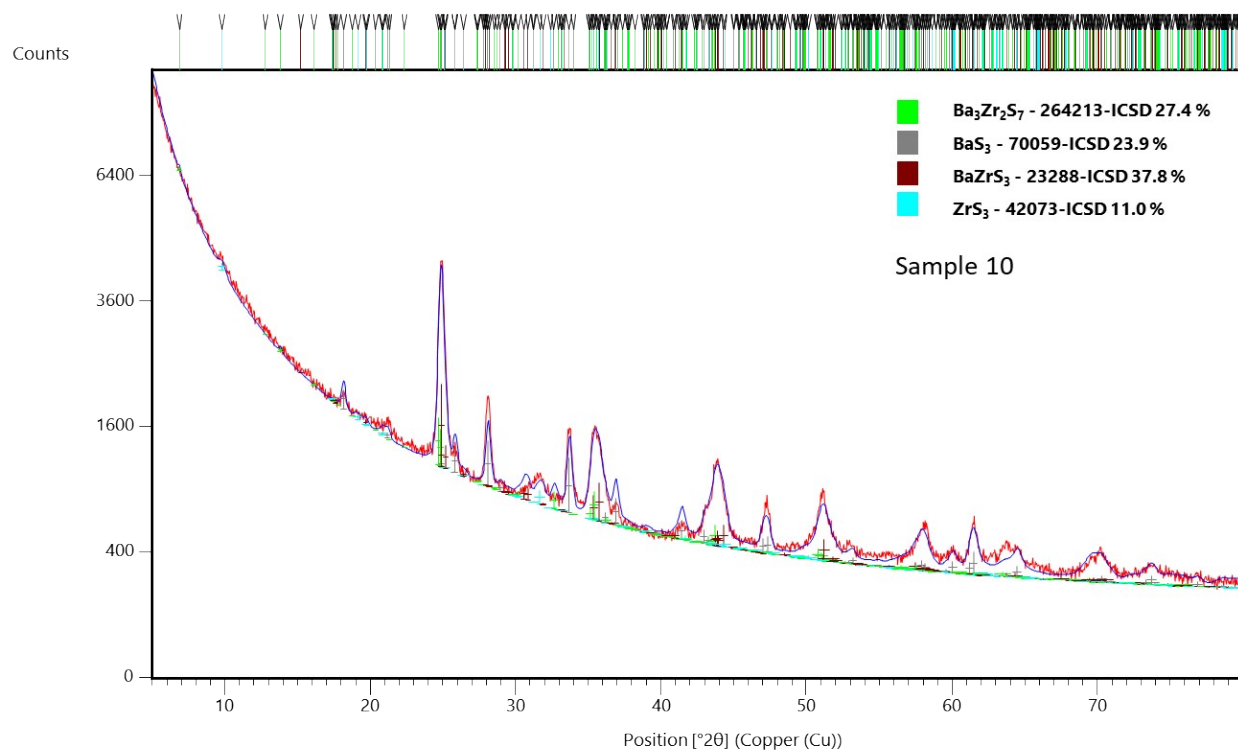


**Figure S12:** Rietveld refinement for Sample 10 synthesized from method 2 described in the main text. The XRD pattern collected was found to be accounted for by 37.8%  $BaZrS_3$ , 27.4% RP phases  $Ba_3Zr_2S_7$ , 23.9%  $BaS_3$ , and 11%  $ZrS_3$ .

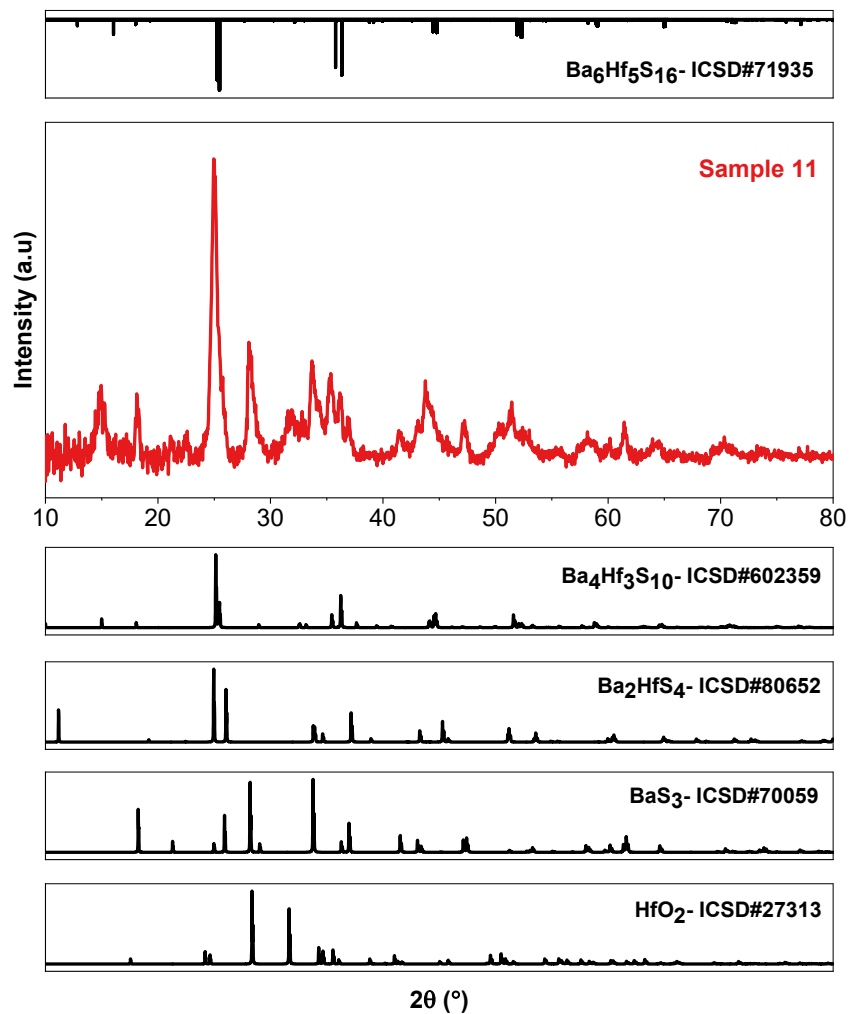


**Figure S13:** XRD pattern for Ba-Hf-S film from hybrid precursor route sulfurized for 15 min at 575 °C with 0.07 atm sulfur pressure.

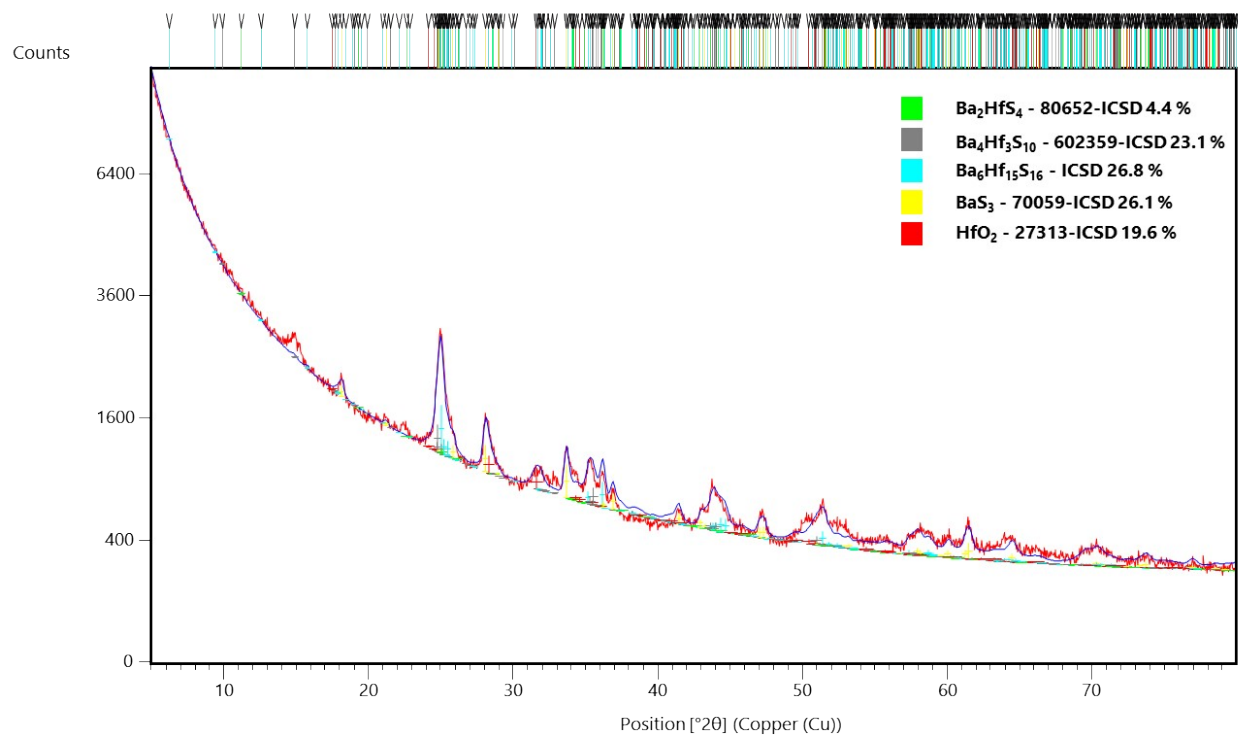


**Figure S14:** Rietveld refinement for Ba-Hf-S film from hybrid precursor route sulfurized for 15 min at 575 °C with 0.07 atm sulfur pressure. The XRD pattern collected was found to be accounted for by 26.8% Ba<sub>6</sub>Hf<sub>15</sub>S<sub>16</sub>, 23.1% Ba<sub>4</sub>Hf<sub>3</sub>S<sub>10</sub>, 4.4% Ba<sub>2</sub>HfS<sub>4</sub>, 26.1% BaS<sub>3</sub>, and 19.6% HfO<sub>2</sub>.

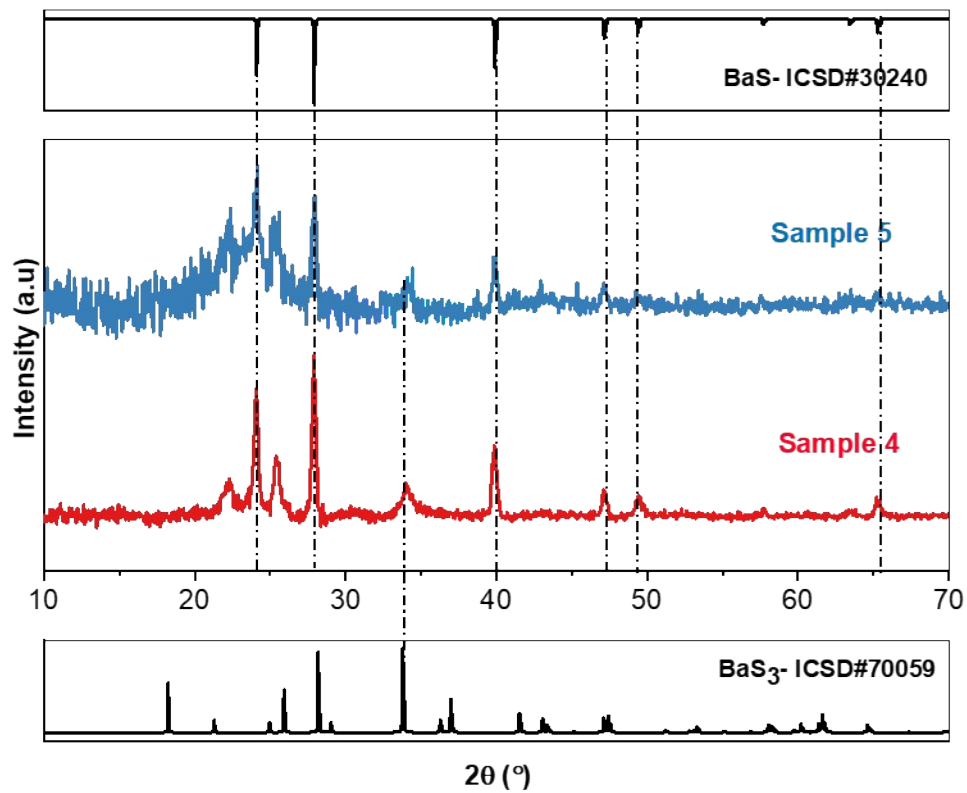


**Figure S15:** XRD patterns of Ba-Zr-S films synthesized as described in Method 1 followed by 1 h sulfurization heat treatments at 575 °C in evacuated 5 mL ampules containing 0.03 mmol HfH<sub>2</sub> and 0.06 mmol sulfur in Sample 4 and 0.03 mmol in Sample 5.

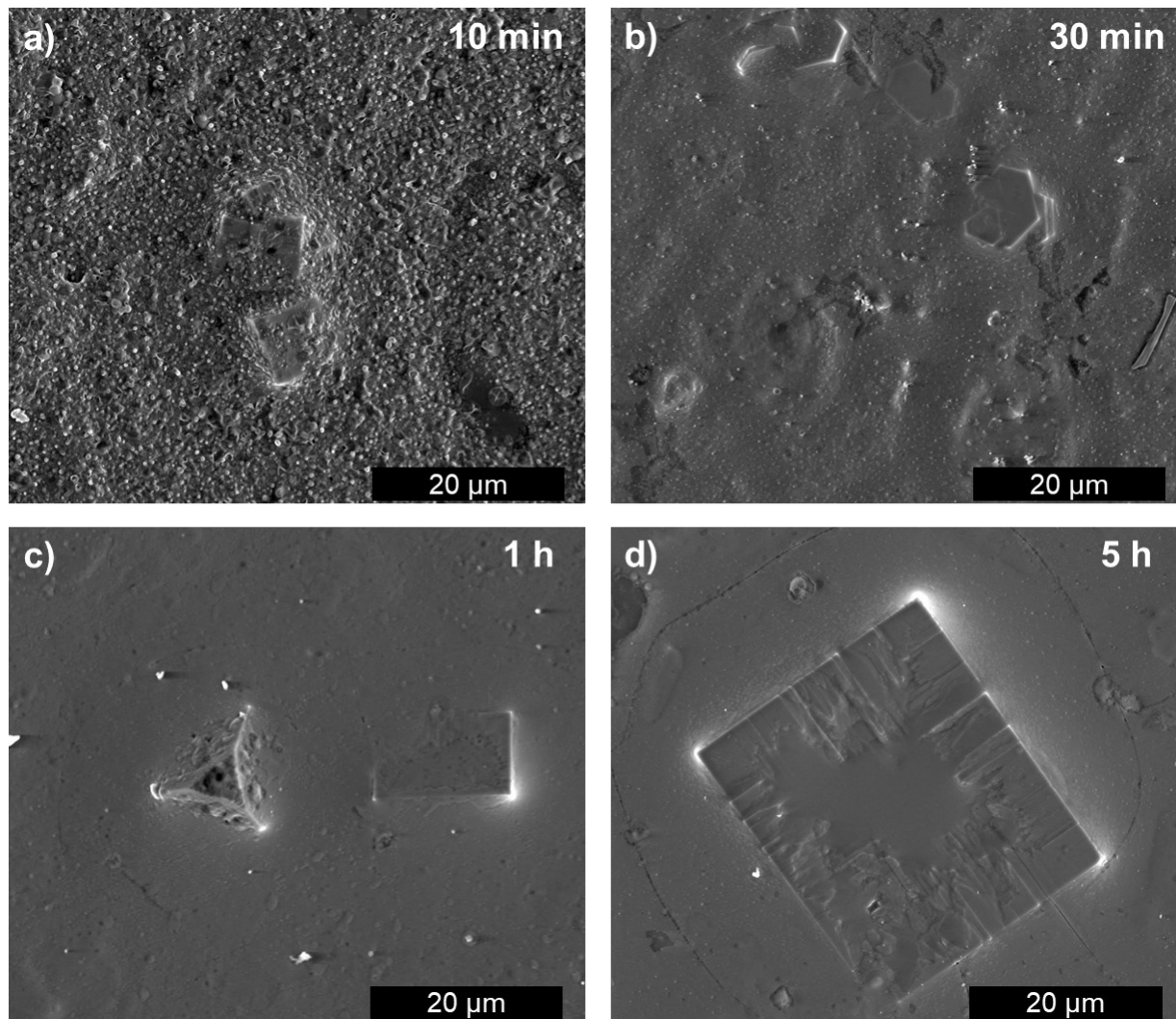


**Figure S16:** Ba-Zr-S films created utilizing Method 3 and heat treated in 5 mL borosilicate ampules containing 0.1 mmol sulfur powder and no  $\text{HfH}_2$  at 575 °C for times ranging from 10 minutes to 5 hours excluding furnace heat up time. **a)** shows 5 to 10  $\mu\text{m}$  cubic crystals of  $\text{BaZrS}_3$  buried under amorphous material. **b)** shows 10 to 15  $\mu\text{m}$  crystals of  $\text{BaZrS}_3$  surrounded by amorphous material. **c)** shows two 10 to 15  $\mu\text{m}$   $\text{BaZrS}_3$  crystals surrounded by amorphous material. **d)** shows a large  $\sim 30 \mu\text{m}$  cubic crystal of  $\text{BaZrS}_3$  surrounded by amorphous material.

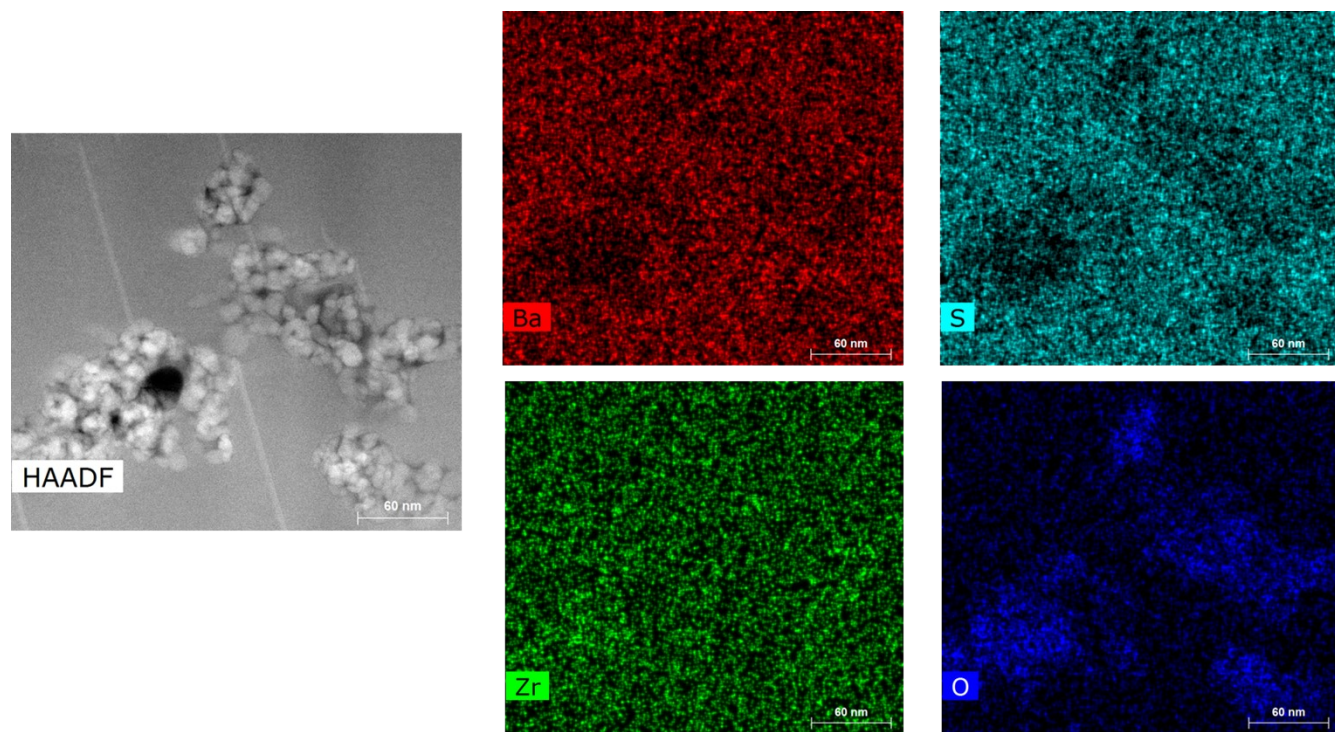


**Figure S17:** STEM-HAADF image and the EDX maps of a bright spot in the  $\text{BaZrS}_3$  grain synthesized from sulfurizing  $\text{BaZrO}_3$  film at  $575^\circ\text{C}$  for 24 h with sulfur in the presence of  $\text{HfH}_2$ .

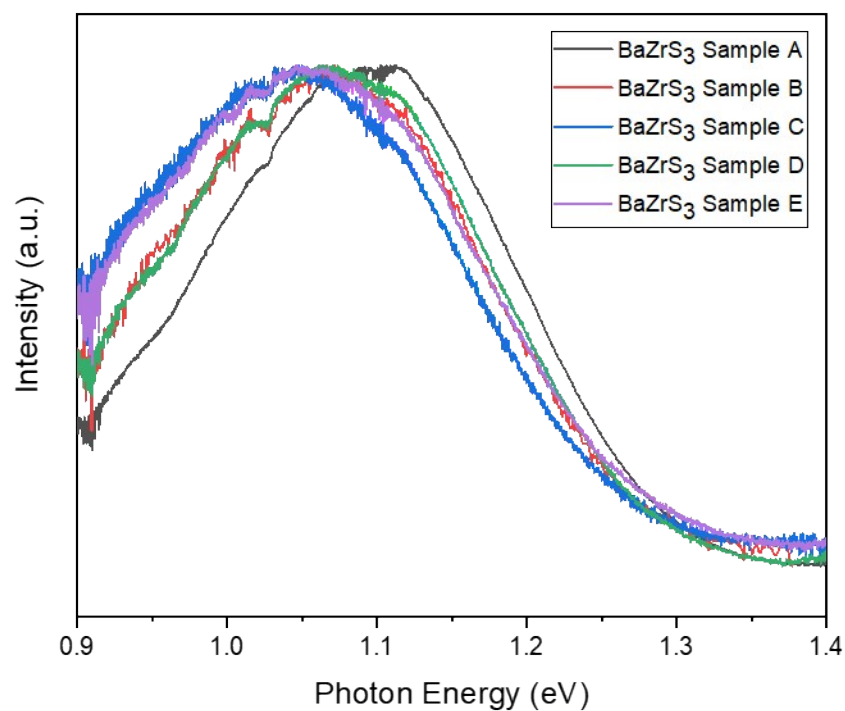


**Figure S18:** Photoluminescence (PL) spectrum of Ba-Zr-S samples synthesized from different routes. Sample A is the BaZrS<sub>3</sub> film produced from sulfurizing BaZrO<sub>3</sub> film with sulfur in the presence of HfH<sub>2</sub> at 575 °C for 24 h. Sample B is the BaZrS<sub>3</sub> film achieved from hybrid precursor ink containing Cp\*<sub>2</sub>Ba and ZrH<sub>2</sub>, where the as-drop casted film was sulfurized with sulfur at 575 °C for 1h. Sample C is the BaZrS<sub>3</sub> powder synthesized from BaS and ZrS<sub>2</sub> precursors with I<sub>2</sub> as the transport agent at 575 °C for 12 h. Sample D is the BaZrS<sub>3</sub> powder synthesized from BaS and ZrS<sub>2</sub> precursors with excess sulfur at 575 °C for 12 h. Sample E is the BaZrS<sub>3</sub> powder synthesized from BaS and ZrS<sub>2</sub> precursors with excess selenium flux at 575 °C for 12 h. A strong photoemission is observed between 1.05 eV and 1.1 eV for all the samples.

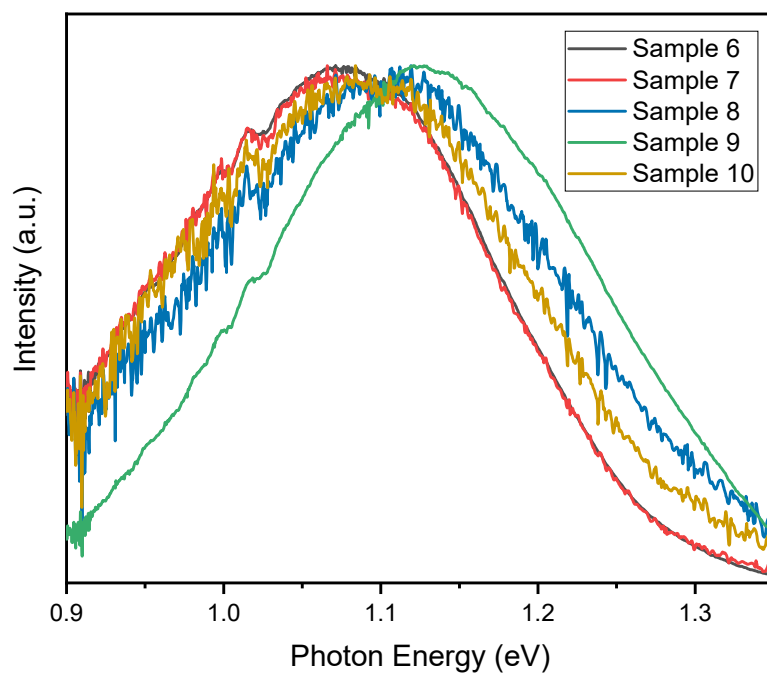


**Figure S19:** Photoluminescence (PL) spectra of Ba-Zr-S samples synthesized from hybrid precursor route. The samples 6-10 are described in the main text. A strong photoemission is observed between 1.05 eV and 1.15 eV for all the samples.

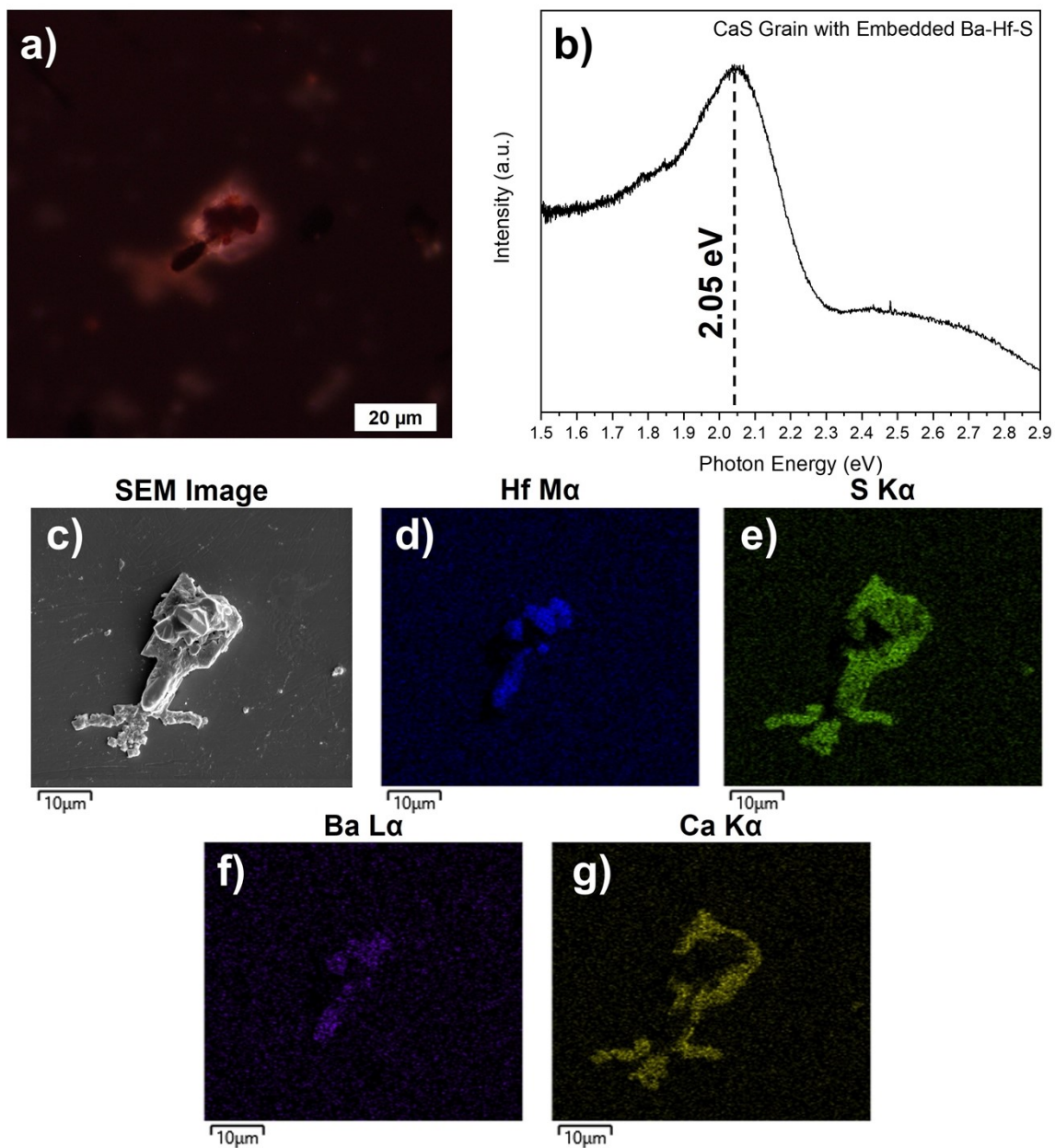


**Figure S20:** **a)** PL image of a CaS grain with embedded Ba-Hf-S made on an Eagle XG substrate as described in Method 5 and sulfurized in a 5 mL ampule with 0.30 mmol S and 0.03 mmol HfH<sub>2</sub> for 10 days at 575 °C. **b)** a PL spectrum of the luminescent grain peaks at 2.05 eV with shoulders at lower and higher energies. **c)** an SEM image of the same luminescent grain. **d)-g)** EDX maps of the SEM show that the luminescent areas in the grain in S6a are CaS, while the dark areas are Ba-Hf-S.

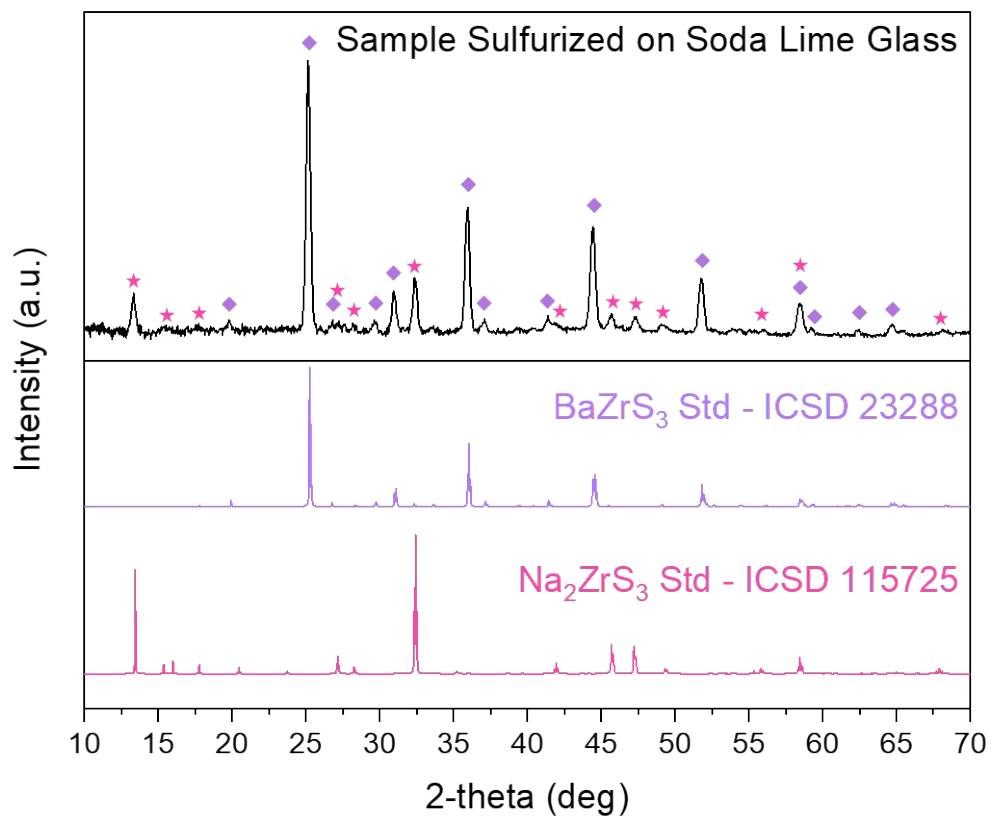


**Figure S21:** XRD pattern of a BaZrS<sub>3</sub> film created as described in Method 1 on soda-lime glass after a 3 h sulfurization heat treatment shows the formation of a Na<sub>2</sub>ZrS<sub>3</sub> secondary phase due to Na<sup>+</sup> diffusion from the SLG substrate. Purple diamonds correspond to BaZrS<sub>3</sub> peaks, and magenta stars correspond to Na<sub>2</sub>ZrS<sub>3</sub> peaks.

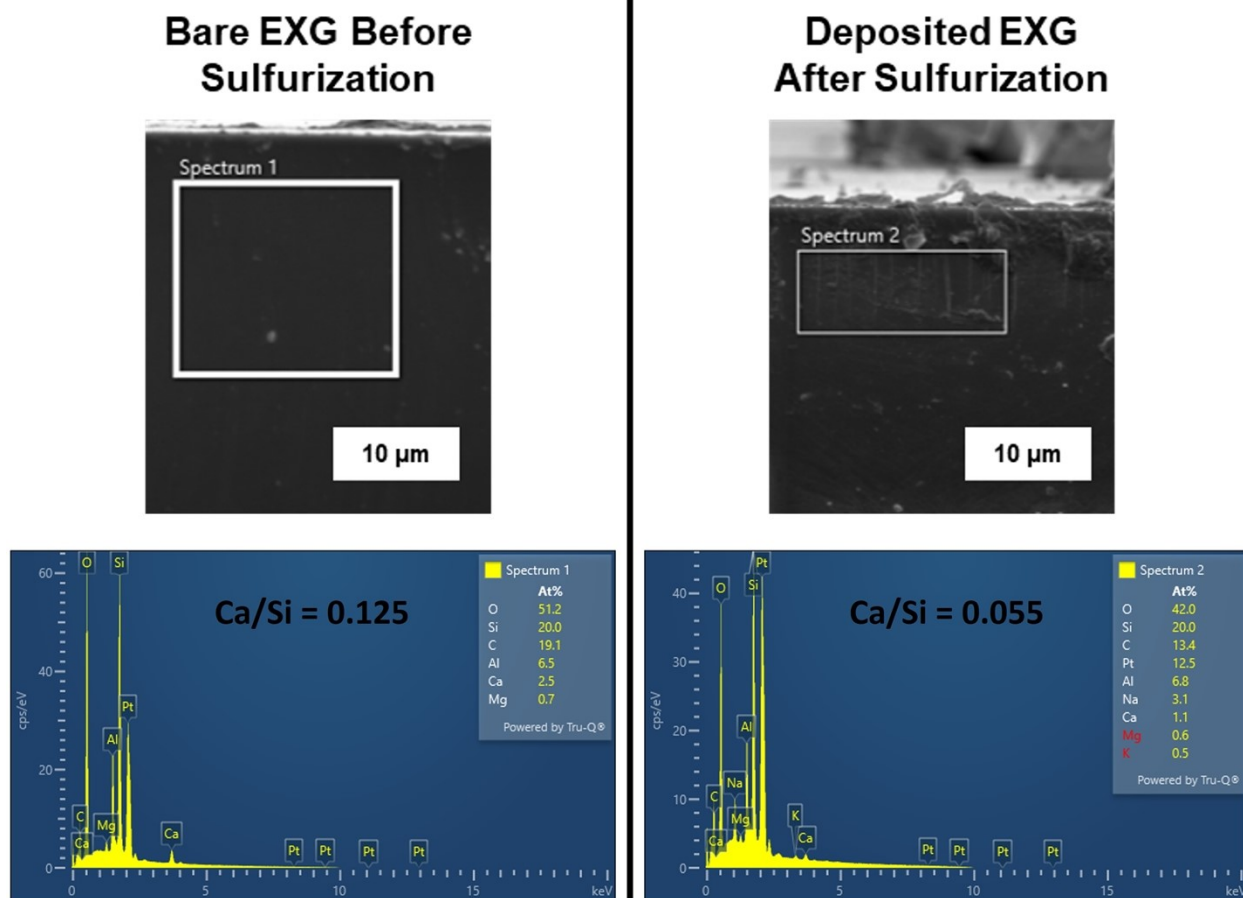


**Figure S22:** SEM-EDX spectra collected on a side-view image of bare Eagle XG (EXG) glass substrate before sulfurization and on an EXG substrate on which Ba-Zr-S was deposited and the substrate was sulfurized in a 5 mL ampule with 0.30 mmol S and 0.03 mmol HfH<sub>2</sub> for 10 days at 575 °C. The substrate was fractured in the middle to expose bulk glass after sulfurization heat treatment was complete. The Ca in the substrate after sulfurization is significantly lower than before sulfurization as indicated by the calcium to silicon ratio in the glass.

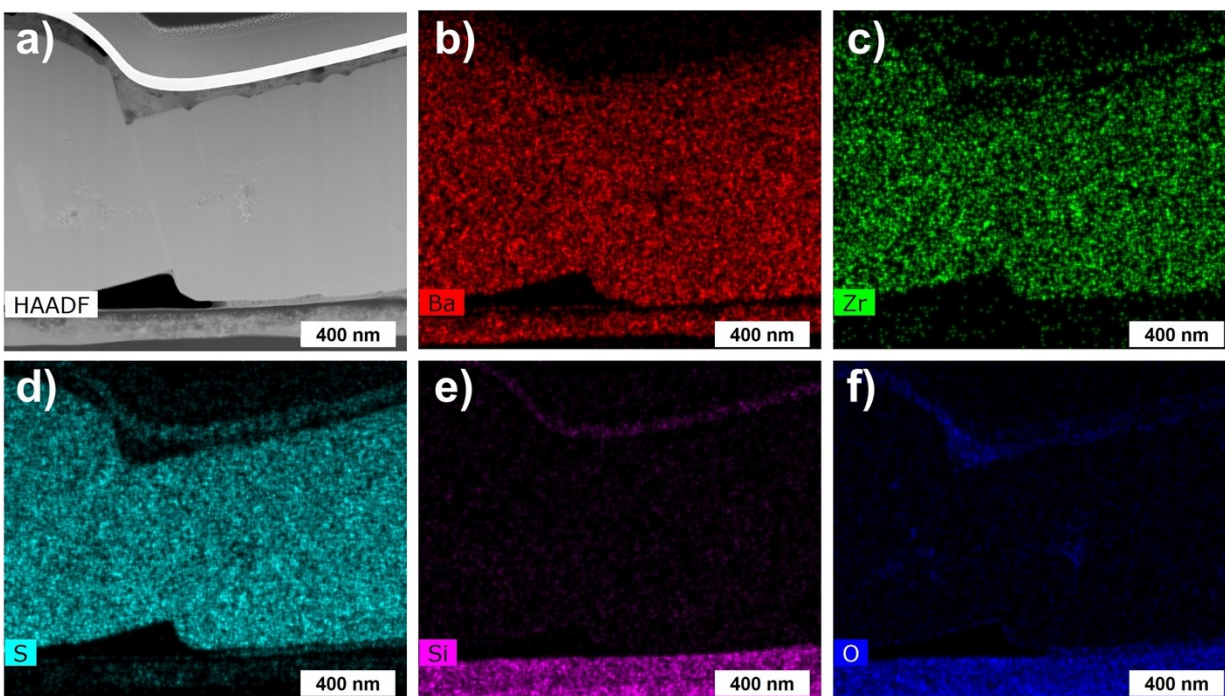


**Figure S23:** a) STEM HAADF image of a lamella of a BaZrS<sub>3</sub> grain synthesized as described in Method 4 involving a 12 h, 700 °C heat treatment step in air to form BaZrO<sub>3</sub> and sulfurized for 24 h at 575 °C in a 5 mL ampule containing 0.31 mmol S and 0.05 mmol HfH<sub>2</sub>. The lamella contains a piece of the quartz substrate that the film was coated on. b)-f) STEM-EDX maps show that barium has diffused into the quartz substrate.

## Supplementary Information References

- (1) Pandey, J.; Ghoshal, D.; Dey, D.; Gupta, T.; Taraphder, A.; Koratkar, N.; Soni, A. Local Ferroelectric Polarization in Antiferroelectric Chalcogenide Perovskite BaZrS<sub>3</sub> Thin Films. *Phys Rev B* **2020**, *102* (20), 205308. <https://doi.org/10.1103/PhysRevB.102.205308>.
- (2) Niu, S.; Milam-Guerrero, J.; Zhou, Y.; Ye, K.; Zhao, B.; Melot, B. C.; Ravichandran, J. Thermal Stability Study of Transition Metal Perovskite Sulfides. *J Mater Res* **2018**, *33* (24), 4135–4143. <https://doi.org/10.1557/jmr.2018.419>.
- (3) Kayastha, P.; Tiwari, D.; Holland, A.; Hutter, O. S.; Durose, K.; Whalley, L. D.; Longo, G. High-Temperature Equilibrium of 3D and 2D Chalcogenide Perovskites. *Solar RRL* **2023**, 2201078. <https://doi.org/10.1002/solr.202201078>.